



CHORUS

This is the accepted manuscript made available via CHORUS. The article has been published as:

Critical transitions in heterogeneous networks: Loss of low-degree nodes as an early warning signal

Alessandro Loppini, Simonetta Filippi, and H. Eugene Stanley

Phys. Rev. E **99**, 040301 — Published 2 April 2019

DOI: [10.1103/PhysRevE.99.040301](https://doi.org/10.1103/PhysRevE.99.040301)

1 **Critical transitions in heterogeneous networks:**
2 **loosing of low-degree nodes as an early warning signal**

3 Alessandro Loppini,^{1,*} Simonetta Filippi,^{1,2,†} and H. Eugene Stanley³

4 ¹*Department of Engineering, Campus Bio-Medico University of Rome,*
5 *Via A. del Portillo 21, 00128, Rome, Italy*

6 ²*International Center for Relativistic Astrophysics Network - ICRANet,*
7 *Piazza della Repubblica 10, Pescara I-65122, Italy*

8 ³*Center for Polymer Studies and Department of Physics,*
9 *Boston University, Boston, MA 02215, USA.*

A large number of real networks show abrupt phase transition phenomena in response to environmental changes. In this case, cascading phenomena can induce drastic and discontinuous changes in the system state and lead to collapse. Although complex network theory has been used to investigate these drastic events, we are still unable to predict them effectively. We here analyze collapse phenomena by proposing a minimal two-state dynamic on a complex network and introducing the effect of local connectivities on the evolution of network nodes. We find that a heterogeneous system of interconnected components presents a mixed response to stress and can serve as a control indicator. In particular, before the critical transition point is reached a severe loss of low-degree nodes is observed, masked by the minimal failure of higher-degree nodes. Accordingly, we suggest that a significant reduction in **less connected** nodes can indicate impending global failure.

10 Many natural, economic and social systems
11 exhibit abrupt phase transition phenomena
12 in response to environmental changes [1–11].
13 Examples include epidemic spreading, traffic
14 networks, climatic and ecosystems changes,
15 cells networks, and heart and brain dynam-
16 ics. In this context, complex network theory
17 has been applied to both real and humanly-
18 constructed systems and has provided useful
19 statistical measurements and indicators able
20 to describe such complex phenomena [12–14].
21 Recently a similar approach was used to
22 investigate economic data [15]. It was found
23 that combining a simple dynamics of internal
24 and external failure with a reversal process
25 of recovery in an interacting network reveals
26 critical transitions in the percentage of active
27 nodes and hystereses that cause the phase-
28 flipping phenomena seen in fluctuating stock
29 market indices. That formulation is also able to
30 describe a more general class of processes [15].
31 In this **contribution**, we propose a gener-
32 alization that takes into account network
33 heterogeneity induced by topology, similarly
34 to studies on epidemic spreading [16]. By

35 using this approach, we show that the route
36 towards the critical point is shaped by the
37 connectivity class of the nodes, with significant
38 consequences on the formulation of effective
39 indicators of transition forecasting.

40
41 *Dynamical model on networks.* We consider
42 a two-state dynamic model [15] where an “ac-
43 tive” node can fail either because of internal fac-
44 tors with an intrinsic transition rate p_a or be-
45 cause of external influences with a rate p_s . Ex-
46 ternal failures are due to factors external to the
47 node and occurs when the number of its failed
48 neighbors exceeds a certain threshold, thus de-
49 noting a compromised functionality by a loss of
50 feedback in interactions with other nodes. In-
51 ternal failure occurs when intrinsic stresses ex-
52 ceed a certain level. Nodes recover at a rate
53 p_r when they are able to mitigate destructive
54 functional alterations. Compared to the orig-
55 inal model [15] we introduce an equal mean
56 recovery time from both external and internal
57 failures and use transition rate instead of re-
58 covery time to describe the rescue process as
59 a single transition from failed to active. We

also examine heterogeneity in node connectivity. Specifically, the effective rate of a node's external failure takes into account the degree-dependent probability that it will be exposed to a fraction of failed nodes that exceeds a threshold. The threshold value depends on network degree, i.e., a damaged neighborhood must be defined locally with respect to the original local connectivity. In our model, we set this threshold at 50% of the node's original neighborhood size, based on the hypothesis that a particular node is insensitive to extrinsic failure if at least half of its neighbors are safe. Slight variations of this threshold don't alter our analysis significantly. This approach models several dynamical processes occurring in real networks, from the functional regulation of interacting cells, to epidemic and information spreading, to financial markets crashes [15, 17, 18]. In addition, the proposed model shares similarities with the Watts model and with other generalizations analyzing cascades in networks with no intrinsic failure and recovery dynamics, and with homogenous and normally distributed thresholds [19–21].

Mean-field theory. By adopting a mean-field approach it is possible to write a **balance** equation that regulates the dynamics of the fraction of active nodes for each degree class,

$$\frac{df_A^k(t)}{dt} = p_r(1 - f_A^k(t)) - (p_a + p_s R_k) f_A^k(t), \quad (1)$$

where f_A^k is the fraction of active nodes in the k -th class and R_k is the average probability that the neighborhood of a node of degree k is damaged. This factor takes into account the effective probability θ_k that a node of degree k connects to a failed neighbor and all the configurations in which the number of active neighbors is less than or equal to the threshold $m(k) = k/2$ (rounded down to the nearest integer), i.e. $R_k = \sum_{j=0}^{m(k)} \binom{k}{k-j} \theta_k^{k-j} (1 - \theta_k)^j$, with $\theta_k = \sum_{k'} P(k'|k) f_{F_n}^{k'}$ and $f_F^k = 1 - f_A^k$. By definition, $P(k'|k)$ is the probability that a node of degree k is connected to a node of degree k' . **Notably**, $f_{F_n}^k$ represents the fraction of

failed neighbors of degree k , i.e. the probability that a node of degree k is failed conditioned on one of its neighbor being active [20]. This is a dynamical variable satisfying Eq. (1) with $R_k = \sum_{j=0}^{m(k)-1} \binom{k-1}{k-j-1} \theta_k^{k-j-1} (1 - \theta_k)^j$. Taking into account all degree classes in the network and considering both reference nodes and neighbors, Eq. (1) is a dynamical system of order $2k$. It is convenient to rewrite equation (1) by multiplying both sides by $1/p_a$ and by rescaling the time to be dimensionless from $\tau = p_a t$,

$$\frac{df_A^k(\tau)}{d\tau} = \tilde{p}_r(1 - f_A^k(\tau)) - (1 + \tilde{p}_s R_k) f_A^k(\tau), \quad (2)$$

where $\tilde{p}_r = p_r/p_a$ and $\tilde{p}_s = p_s/p_a$. We investigate system behavior by analyzing steady-state active fractions of nodes for each connectivity class, by varying the dimensionless parameters \tilde{p}_r and \tilde{p}_s , i.e. at different grades of internal and external failures occurrence, and recovery capacity. In particular, we numerically compute fixed points of Eq. (1) by slowly varying the control parameter \tilde{p}_r both for positive (increments) and negative (decrements) directions at different and constant values of \tilde{p}_s . Fixed points calculated at \tilde{p}_r^n are used as the initial guess at \tilde{p}_r^{n+1} . We test the behavior of the model in (i) a random network, (ii) a scale-free topology, (iii) a spatially-embedded network extracted from a finite set of nodes and shaped by nearest-neighbors interactions. We select these architectures because real networks are usually heterogeneous and exhibit features common to both random and regular networks or may show scale-free features such as hubs.

Random networks. We consider a Poisson degree distribution characterized by $P(k) = e^{-\langle k \rangle} \langle k \rangle^k / k!$, and by a conditional degree distribution $P(k'|k) = k' P(k') / \langle k \rangle$, peculiar of uncorrelated networks. We set the mean degree of network $\langle k \rangle = 10$ in our calculations, and restrict our analysis to $k \leq 25$ because this allows us to include the most significant fraction of nodes (the distribution rapidly goes to zero when $k > \langle k \rangle$). Figure 1A shows

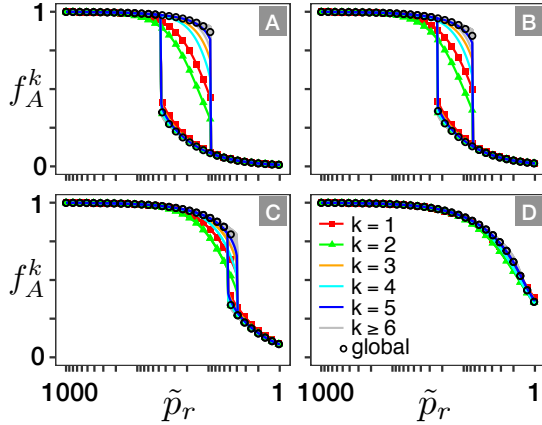


Figure 1. Active fraction of nodes in a random uncorrelated network computed by varying the parameter $\tilde{p}_r = p_r/p_a$ at different values of $\tilde{p}_s = p_s/p_a$. (A) $\tilde{p}_s = 100$. (B) $\tilde{p}_s = 50$. (C) $\tilde{p}_s = 10$. (D) $\tilde{p}_s = 1$. Colored curves represent the active fraction of nodes for different connectivity classes of nodes. Markers represent the total active fraction of nodes in the network computed as $\sum_k P(k)f_A^k$. High values of spreading parameter show discontinuous transitions before which a significant loss of low-degree nodes can be observed.

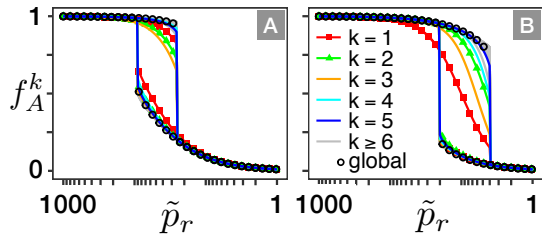


Figure 2. Active fraction of nodes at different threshold values in a random uncorrelated network, computed by varying the parameter $\tilde{p}_r = p_r/p_a$ at $\tilde{p}_s = 100$. (A) $m(k) = 2k/3$. (B) $m(k) = k/3$. Colored curves represent the active fraction of nodes for different connectivity classes of nodes. Markers represent the total active fraction of nodes in the network computed as $\sum_k P(k)f_A^k$. Transition point in (A) and (B) occurs at lower and higher values of the spreading parameter, respectively, compared to $m(k) = k/2$, because of a lower or higher resistance of nodes to neighbors failure. In both cases, a significant loss of low-degree nodes can be observed before the abrupt transition.

that at $\tilde{p}_s = 100$ the system undergoes a clear
 146 discontinuous abrupt transition and hysteresis.
 147 Note that each node subpopulation approaches
 148 the discontinuity point differently. Low-degree
 149 nodes show a smooth and strong decline in their
 150 fraction of active units. High-degree nodes re-
 151 main strong until they reach the critical point.
 152 In the extreme cases of $k = 1, 2$ approximately
 153 50-70% of nodes are in a failed state prior to
 154 the transition point. Figures 1B, 1C, and 1D
 155 show that this behavior is qualitatively main-
 156 tained at lower values of \tilde{p}_s , i.e., at lower values
 157 of the external failure rate, although the transi-
 158 tion point shifts at lower recovery rate values.
 159 When $\tilde{p}_s = 1$ the transition is smooth for all
 160 node subpopulations. When we consider the
 161 global behavior of the ensemble, by computing
 162 the total fraction of active nodes in the network
 163 as $f_A = \sum_k P(k)f_A^k$, the differences disappear
 164 (black markers in Figure 1). The total active
 165 fraction is discontinuous in the asymptotic solu-
 166 tions at high values of the spreading term and
 167 shows small variations prior to the transition,
 168 which reproduces the behavior of high-degree
 169 nodes. The partial smoothing of the global
 170 steady-state solutions as a function of the control
 171 parameter before the transition point is pri-
 172 marily due to the leaf ($k = 1$) and less con-
 173 nected nodes ($k < 6$), as was found in the local
 174 analysis. Results computed at different values of
 175 the threshold $m(k) = 2k/3, k/3$ (rounded down
 176 to the nearest integer) show that this behavior
 177 is qualitatively conserved also when nodes are
 178 more or less resistant to neighbors failure (Fig-
 179 ure 2), despite a shift of the transition point at
 180 lower and higher values of the spreading param-
 181 eter, respectively.

183 *Scale-free networks.* We further investigate
 184 model behavior in a scale-free topology. In this
 185 case we consider a degree distribution $P(k) =$
 186 $k^{-\gamma}$ with $\gamma = 3$. A finite-size network of 10000
 187 nodes constructed with similar parameters by
 188 using the BA algorithm [22] showed a maxi-
 189 mum degree of about 50. Therefore we use
 190 this cutoff in the mean-field description with
 191 the aim to keep low the dimensionality of the

192 dynamical system and the computational cost.
 193 We also assume an uncorrelated network and
 194 adopt the same conditional degree distribution
 195 used in the random case. Active fractions of
 196 nodes in scale-free topology do not show abrupt
 197 transitions also in case of high probabilities of
 198 failures spreading (see Fig. 3A). However, it is
 199 still possible to observe a larger reduction in
 200 the partial fractions of active nodes within the
 201 low-connectivity classes compared to the highly
 202 connected ones. **Interestingly**, in this case, these
 203 larger reductions are not masked when observ-
 204 ing the global behavior of the network. In fact,
 205 the total fraction of active nodes mostly repre-
 206 sents the behavior of less connected nodes which
 207 are much more abundant than hubs in scale-free
 208 networks. **Results obtained with a cutoff of**
 209 **$k = 100$ and $k = 200$ do not show significant**
 210 **differences (see Fig.s 3B and 3C).**

212 *Spatially-embedded regular networks.* We fi-
 213 nally determine model solutions in the non-
 214 random regular networks typical in interact-
 215 ing space-embedded systems in which units are
 216 physically connected. **In particular, we build**
 217 **a spatially-embedded network starting from a**
 218 **cubic lattice, fixing a three-dimensional Moore**
 219 **neighborhood of range 1 to set the connections.**
 220 **Then, we randomly remove links with $p_l=0.3$ to**
 221 **induce heterogeneities. Such topological prop-**
 222 **erties resemble** the biological architecture of β -
 223 cell networks in endocrine pancreatic islets, an
 224 emblematic case in which communications are
 225 key in shaping emergent dynamics, cell func-
 226 tion, and fate [23–30]. Note that this architec-
 227 ture can be representative of many other sys-
 228 tems in which physical constraints shape net-
 229 work topology, such as highways, water distri-
 230 bution, and power grid networks. The resulting
 231 graph is a spatial network of $\simeq 11000$ nodes
 232 with a maximum of 26 neighbors per node. We
 233 compute statistics of the network using normal-
 234 ized frequency of nodes degree and normalized
 235 edge frequency between nodes of degree k and
 236 k' . Each conditional probability $P(k'|k)$ is nor-
 237 malized at 1. Figure 3D shows that prior to the
 238 transition point when the recovery rate values

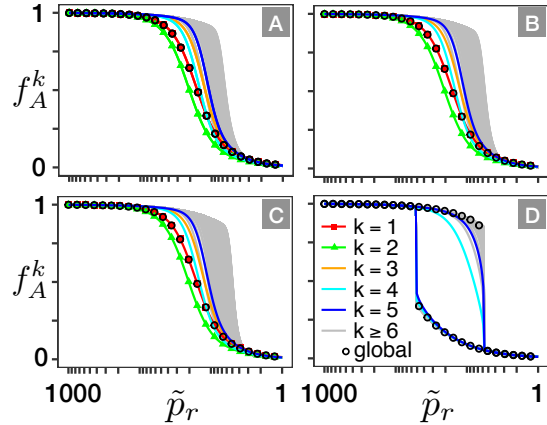


Figure 3. Active fraction of nodes computed by varying the parameter $\tilde{p}_r = p_r/p_a$ at $\tilde{p}_s = 100$. (A) Scale-free uncorrelated network (cutoff $k = 50$). (B) Scale-free uncorrelated network (cutoff $k = 100$). (C) Scale-free uncorrelated network (cutoff $k = 200$). (D) Spatially-embedded network (degree distribution and conditional degree distribution calculated from a finite-size network, see text). Colored curves represent the active fraction of nodes for different connectivity classes of nodes. Markers represent the total active fraction of nodes in the network computed as $\sum_k P(k)f_A^k$. The scale-free topology do not show abrupt transition in contrast to the spatially-embedded one. Larger variations in low degree nodes compared to high-degree nodes can be observed in both cases.

239 are decreasing, the active fraction of low-degree
 240 nodes (here $k = 4$ is the lowest degree) changes
 241 smoothly and more quickly than in high-degree
 242 nodes, in line with random and scale-free uncor-
 243 related networks. At the transition point when
 244 the network globally collapses, the active frac-
 245 tion of all node classes becomes discontinuous.
 246 In line with the random network, the total frac-
 247 tion of active nodes is representative of the high-
 248 degree nodes of the network, while the larger
 249 reductions in the active fraction of lower degree
 250 nodes are masked.

251 *Validation of mean-field analysis.* To check
 252 whether mean-field theory correctly describes
 253 real networks behavior, we further simulated
 254 the two-state dynamical model in three finite-

size networks of 10000 nodes (11056 for the spatially-embedded case) characterized by the three topologies discussed above. In this case, the stochastic nature of the process is not smoothed by the thermodynamic limit. In particular, numerical simulations are performed via random evolutions of the networks by using a Monte Carlo method. All nodes are initialized in an active or failed state depending on the initial value of the parameter \tilde{p}_r and on the direction of variation: failed state for low \tilde{p}_r and increments of the parameter, active state for high \tilde{p}_r and decrements of the parameter. To compute steady-state average fractions of nodes we adiabatically changed the control parameter and calculated the time-averaged numbers of active nodes within each connectivity class at every step, discarding a proper initial period to avoid the effect of transient responses on steady-states estimates. We then used the final state of the network to set the initial state at the next \tilde{p}_r value. Numerical simulations confirmed the results obtained with the mean-field analysis (Fig. 4). When varying the control parameter, the active fractions of nodes show fluctuations around a smoothly varying mean value that follows the mean-field solutions for all the connectivity classes. Although the critical point is slightly shifted at lower values of the control parameter, the emergent phenomena are qualitatively unchanged.

Our results show that adding heterogeneity to the mathematical representation of a dynamical network produces a qualitatively different response from each connectivity class of nodes. The leaf and less connected nodes display an emergent behavior similar to that in sparse topologies, and highly-clustered nodes display abrupt transitions in their active fraction that resemble the global behavior of strongly connected networks responding to changes in control parameters. This is in line with the increased failure probability of low degree nodes in small cascade regimes and with hysteresis observed in similar threshold models [20, 21]. Although, these formulations do not include recov-

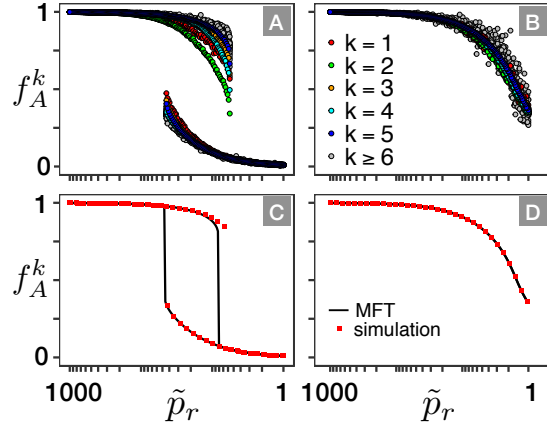


Figure 4. Active fraction of nodes numerically computed in a finite-size ($N = 10000$) random uncorrelated network computed by varying the parameter $\tilde{p}_r = p_r/p_a$ at different values of $\tilde{p}_s = p_s/p_a$. (A) $\tilde{p}_s = 100$. (B) $\tilde{p}_s = 1$. (C) Comparison of global behavior between numerical simulations and mean-field at $\tilde{p}_s = 100$. (D) Comparison of global behavior between numerical simulations and mean-field at $\tilde{p}_s = 1$. Colored points in (A) and (B) denote the active fraction of nodes for different classes of nodes. Black curves and red squares in (C) and (D) represent the total active fraction of nodes in the network for mean-field and simulations, respectively, computed as $\sum_k P(k)f_A^k$.

ery and intrinsic failure and are based on different threshold rules. Our results are also similar to the original Watts model [19] in case of large extrinsic failure probability, where threshold has significant effects. It is worth mentioning that, in our case, fixing the threshold to $k/2$ rounded down induces asymmetry between even and odd degrees in the partial active fraction of nodes. In particular, our choice makes odd degree nodes to be susceptible to external failure at more than 50% of failed neighbors. Instead, even nodes became susceptible exactly at 50% of failed neighbors and, thus, are more likely to fail. The asymmetry changes by setting the threshold to $k/3$ or $2k/3$, and this is again mostly linked to the percentage of neighbors which have to be failed to make the

319 **node susceptible**. Notably, while in scale-free
 320 networks the global fraction of active nodes is
 321 strongly representative of less connected nodes,
 322 in random and spatially-embedded networks the
 323 opposite holds, and large reductions in **less con-**
 324 **connected** nodes are masked in the global response.
 325 In these specific cases, relying on a global indi-
 326 cator of network functionality, such as the
 327 total fraction of active nodes, is likely to be
 328 misleading and can significantly underestimate
 329 failure risk and the probability of critical col-
 330 lapses. Indicators of catastrophic transitions
 331 based on slowing down of the recovery dynam-
 332 ics from perturbations and flickering phenom-
 333 ena in the state of the system have been pro-
 334 posed in the literature [31, 32]. In particular,
 335 they were applied to the identification of catas-
 336 trophic changes in climate, ecologic mutualistic
 337 communities, and depression development [33–
 338 35]. These dynamical indicators have a differ-
 339 ent nature compared to the steady-states here
 340 analyzed, which instead are not dynamical by
 341 definition. **However, they are strictly linked to**
 342 **critical bifurcation points and bistability of the**
 343 **dynamical system and, thus, to the underlying**
 344 **steady solutions on which we based our anal-**
 345 **ysis**. Here we suggest that monitoring **loss in**
 346 **leaf and less connected nodes** in networks show-
 347 ing critical discontinuous transitions gives addi-
 348 tional perspectives on catastrophic failure pre-
 349 diction. Moreover, if the intrinsic dynamics of
 350 the network is considerably faster than the char-
 351 acteristic time which rules stressful parameters
 352 variation, time-window measures of the average
 353 active fraction on nodes based on their connec-
 354 tivity class have the potential to be adopted in
 355 a dynamical perspective. Future investigations
 356 will be devoted to a detailed time-analysis using
 357 predictive indicators based on the observed phe-
 358 nomena, as well as testing the effects of other
 359 threshold rules and nodes correlation [36, 37].
 360 In conclusion, our results reveal that losing **leaf**
 361 **and less connected nodes** in response to stress
 362 may be a general feature of complex systems
 363 characterized by dynamical units whose behav-
 364 ior is regulated in heterogeneous complex net-

365 works. **Based on the very general dynamics used**
 366 **to model nodes evolution, we believe that the**
 367 **observed behavior has potential impacts on un-**
 368 **derstanding the response of several natural and**
 369 **artificial systems upon degradation, and it will**
 370 **encourage expanded research investigating such**
 371 **possibility in real scenarios.**

372 A.L. and S.F. acknowledge the support from
 373 the International Center for Relativistic As-
 374 trophysics Network (ICRANet) and Gruppo
 375 Nazionale per la Fisica Matematica (GNFM-
 376 INdAM). The Boston University Center for
 377 Polymer Studies is supported by NSF Grants
 378 PHY-1505000, CMMI-1125290, and CHE-
 379 1213217, and by DTRA Grant HDTRA1-14-1-
 380 0017.

381 * Corresponding author; a.loppini@unicampus.it

382 † Corresponding author; s.filippi@unicampus.it

- 383 [1] V. Colizza, R. Pastor-Satorras, and A. Vespig-
 384 nani, *Nature Physics* **3**, 276 (2007).
 385 [2] W. Wang, M. Tang, H. E. Stanley, and L. A.
 386 Braunstein, *Reports on Progress in Physics* **80**,
 387 036603 (2017).
 388 [3] Q.-H. Liu, L.-F. Zhong, W. Wang, T. Zhou,
 389 and H. Eugene Stanley, *Chaos: An Inter-*
 390 *disciplinary Journal of Nonlinear Science* **28**,
 391 013120 (2018).
 392 [4] Z. Su, W. Wang, L. Li, J. Xiao, and H. E.
 393 Stanley, *Scientific Reports* **7**, 6103 (2017).
 394 [5] K. Kiyono, Z. R. Struzik, and Y. Yamamoto,
 395 *Physical Review Letters* **96**, 068701 (2006).
 396 [6] T. M. Lenton, H. Held, E. Kriegler, J. W. Hall,
 397 W. Lucht, S. Rahmstorf, and H. J. Schellnhu-
 398 ber, *Proceedings of the National Academy of*
 399 *Sciences* **105**, 1786 (2008).
 400 [7] T. Nagatani, *Reports on Progress in Physics*
 401 **65**, 1331 (2002).
 402 [8] D. Li, B. Fu, Y. Wang, G. Lu, Y. Berezin, H. E.
 403 Stanley, and S. Havlin, *Proceedings of the Na-*
 404 *tional Academy of Sciences* **112**, 669 (2015).
 405 [9] K. Kiyono, Z. R. Struzik, N. Aoyagi, F. Togo,
 406 and Y. Yamamoto, *Physical Review Letters* **95**,
 407 058101 (2005).
 408 [10] H. Stanley, L. Amaral, S. V. Buldyrev,
 409 P. Gopikrishnan, V. Plerou, and M. Salinger,
 410 *Proceedings of the National Academy of Sci-*

- ences **99**, 2561 (2002).
- [11] F. Morone, K. Roth, B. Min, H. E. Stanley, and H. A. Makse, Proceedings of the National Academy of Sciences **114**, 3849 (2017).
- [12] R. Albert and A.-L. Barabási, Reviews of Modern Physics **74**, 47 (2002).
- [13] S. N. Dorogovtsev, A. V. Goltsev, and J. F. F. Mendes, Reviews of Modern Physics **80**, 1275 (2008).
- [14] A. Giuliani, S. Filippi, and M. Bertolaso, Frontiers in Genetics **5**, 83 (2014).
- [15] A. Majdandzic, B. Podobnik, S. V. Buldyrev, D. Y. Kenett, S. Havlin, and H. E. Stanley, Nature Physics **10**, 34 (2014).
- [16] R. Pastor-Satorras and A. Vespignani, Physical Review E **65**, 035108(R) (2002).
- [17] J. E. Trosko, Journal of cell communication and signaling **5**, 53 (2011).
- [18] R. Pastor-Satorras, C. Castellano, P. Van Mieghem, and A. Vespignani, Reviews of modern physics **87**, 925 (2015).
- [19] D. J. Watts, Proceedings of the National Academy of Sciences **99**, 5766 (2002).
- [20] J. P. Gleeson and D. J. Cahalane, Physical Review E **75**, 056103 (2007).
- [21] R. Burkholz, A. Garas, and F. Schweitzer, Physical Review E **93**, 042313 (2016).
- [22] A.-L. Barabási and R. Albert, Science **286**, 509 (1999).
- [23] M. Perez-Armendariz, C. Roy, D. C. Spray, and M. Bennett, Biophysical Journal **59**, 76 (1991).
- [24] M. A. Ravier, M. Güldenagel, A. Charollais, A. Gjinovci, D. Caille, G. Söhl, C. B. Wollheim, K. Willecke, J.-C. Henquin, and P. Meda, Diabetes **54**, 1798 (2005).
- [25] P. Klee, F. Allagnat, H. Pontes, M. Cederroth, A. Charollais, D. Caille, A. Britan, J.-A. Haefliger, and P. Meda, The Journal of Clinical Investigation **121**, 4870 (2011).
- [26] P. Meda, Diabetes **61**, 1656 (2012).
- [27] A. Loppini, A. Capolupo, C. Cherubini, A. Gizzi, M. Bertolaso, S. Filippi, and G. Vitiello, Physics Letters A **378**, 3210 (2014).
- [28] C. Cherubini, S. Filippi, A. Gizzi, and A. Loppini, Physical Review E **92**, 042702 (2015).
- [29] A. Loppini, M. Braun, S. Filippi, and M. G. Pedersen, Physical biology **12**, 066002 (2015).
- [30] A. Loppini, M. G. Pedersen, M. Braun, and S. Filippi, Physical Review E **96**, 032403 (2017).
- [31] M. Scheffer, J. Bascompte, W. A. Brock, V. Brovkin, S. R. Carpenter, V. Dakos, H. Held, E. H. Van Nes, M. Rietkerk, and G. Sugihara, Nature **461**, 53 (2009).
- [32] M. Scheffer, S. R. Carpenter, T. M. Lenton, J. Bascompte, W. Brock, V. Dakos, J. Van de Koppel, I. A. Van de Leemput, S. A. Levin, E. H. Van Nes, *et al.*, Science **338**, 344 (2012).
- [33] V. Dakos, M. Scheffer, E. H. van Nes, V. Brovkin, V. Petoukhov, and H. Held, Proceedings of the National Academy of Sciences **105**, 14308 (2008).
- [34] I. A. van de Leemput, M. Wichers, A. O. Cramer, D. Borsboom, F. Tuerlinckx, P. Kuppens, E. H. van Nes, W. Viechtbauer, E. J. Giltay, S. H. Aggen, *et al.*, Proceedings of the National Academy of Sciences **111**, 87 (2014).
- [35] V. Dakos and J. Bascompte, Proceedings of the National Academy of Sciences **111**, 17546 (2014).
- [36] J. L. Payne, P. S. Dodds, and M. J. Eppstein, Physical Review E **80**, 026125 (2009).
- [37] X.-Z. Wu, P. G. Fennell, A. G. Percus, and K. Lerman, Physical Review E **98**, 022321 (2018).